

Ir d -band Derived Superconductivity in the Lanthanum-Iridium System LaIr_3

Neel Haldolaarachchige,^{1,2} Leslie Schoop,³ Mojammel A. Khan,⁴

Wenxuan Huang,⁵ Huiwen Ji,⁶ Kalani Hettiarachchilage,^{2,7} and David P. Young⁴

¹*Department of Physics and Astronomy, Rowan University, Glassboro, NJ08028, USA*

²*Department of Physics and Engineering, College of Staten Island, CUNY, NY10314, USA*

³*Max-Planck-Institut für Festkörperforschung, Heisenbergstraße 1, D-70569 Stuttgart, Germany*

⁴*Department of Physics and Astronomy, Louisiana State University, Baton Rouge, LA70803, USA*

⁵*Department of Material Science and Engineering,*

Massachusetts Institute of Technology, Cambridge, MA 02142, USA

⁶*Department of Chemistry, Princeton University, Princeton, NJ08540, USA*

⁷*Department of Physics, The College of New Jersey, Ewing, NJ08618, USA*

The electronic properties of the heavy metal superconductor LaIr_3 ($T_c = 3.3$ K) are reported. The estimated superconducting parameters obtained from physical properties measurements indicate that LaIr_3 is a BCS-type superconductor. Electronic band structure calculations show that Ir d -states dominate the Fermi level. A comparison of electronic band structures of LaIr_3 and LaRh_3 shows that the Ir-compound has a strong spin-orbit-coupling effect, which creates a complex Fermi surface.

I. INTRODUCTION

The combination of rare earth and main group transition metal elements can produce compounds with complex, technologically important, and scientifically interesting physical properties. Compounds with $5d$ transition metals show electron correlations and spin-orbit interactions that create interesting electronic properties, such as superconductivity. [1] Only a few Ir compounds are known to display superconductivity and most of their electronic properties are due to the rare earth elements rather than Ir. [2–5] There are, however, a few examples, such as CaIr_2 , IrGe and $\text{Mg}_{10}\text{Ir}_{19}\text{B}_{16}$, where the superconductivity is derived from Ir- d states at the Fermi surface. [6–8] Evens so, there is no simple example of a lanthanide-iridium superconductor whose properties are dominated by Ir- d bands at the Fermi level and strong spin-orbit-coupling.

Here we report the synthesis, experimental superconducting parameters of LaIr_3 and $\text{LaIr}_{2.8}$ and the calculated electronic band structure of LaIr_3 and LaRh_3 . The existence of superconductivity in LaIr_3 has been reported earlier, but besides its superconducting transition temperature T_c , no further characterization is available, except one report on a doping study. [9, 10] LaIr_3 is unusual among the lanthanide superconductors, because it contains $5d$ electrons with no magnetic rare earth ions present. The reported T_c of LaIr_3 is, however, comparable to most Ce $4f$ based superconductors. [12, 13] Still, the superconducting transition temperature of LaIr_3 is much lower than those of the alkaline-based Ir superconductors such as CaIr_2 . [8] The isostructural compound LaRh_3 was also reported to be superconducting with a slightly lower T_c than LaIr_3 of 2.6 K. [14]

II. EXPERIMENT AND CALCULATION

Polycrystalline samples of LaIr_3 were prepared with ultra pure (5N, 99.999%) elemental La and Ir by arc melting. The arc-melted button was sealed inside a quartz tube under vacuum. The tube was then heated (heating rate is 180 °C per hour) to 1000 °C and held at that temperature for about 24 hrs. The quartz tubes with the samples inside were then removed from the furnace and quenched in water. The phase purity and cell parameters of the samples were evaluated by powder X-ray diffraction (PXRD) at room temperature on a Bruker D8 FOCUS diffractometer ($\text{Cu } K_\alpha$). Detailed Rietveld analysis was performed with the MAUD program. [15] The X-ray investigation confirmed that the sample was a single phase with a rhombohedral crystal symmetry with the space group 166 ($R\bar{3}m$). [11] A small amount of pure Ir metal was detected as an impurity, but this had no effect on the observed physical properties of the sample (Ir metal superconduct at very low temperature 0.14K). [16] Further investigation of the sample purity was performed with Energy Dispersive Spectroscopy (EDS) by using a FEI XL30 FEG-SEM system equipped with an EVEX EDS, and confirmed the stoichiometry (ratio of La:Ir) of the sample as 1:3.

The electrical resistivity was measured using a standard four-probe method with an excitation current of 10 mA; small diameter Pt wires were attached to the sample using a conductive epoxy (Epotek H20E). Data were collected from 300 - 2 K and in magnetic fields up to 5kOe using a Quantum Design Physical Property Measurement System (PPMS). The specific heat was measured between 2 and 50 K in the PPMS, using a time-relaxation method at 0 and 5kOe applied magnetic fields. The magnetic susceptibility was measured in a DC field of 10 Oe; the sample was cooled down to 1.8 K in zero-field, the magnetic field was then applied, and the sample magnetization was measured on heating to 4 K [zero-field-cooled (ZFC)], and then on cooling to 1.8 K [field-cooled (FC)]

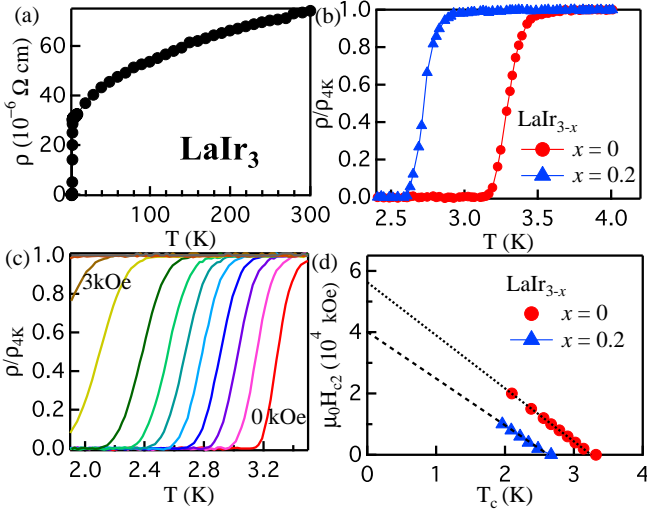


FIG. 1. (Color online) Analysis of the resistivity of LaIr_3 and $\text{LaIr}_{2.8}$. (a) Resistivity at zero applied field. (b) Normalized resistance. (c) Normalized resistance of LaIr_3 with increasing applied magnetic field from 0-3 kOe. (d) The upper critical field as a function of temperature.

in the PPMS.

The electronic structure calculations were performed by density functional theory (DFT) using the WIEN2K code with a full-potential linearized augmented plane-wave and local orbitals [FP-LAPW + lo] basis [17–20] together with the PBE parameterization [21] of the GGA, with and without spin orbit coupling (SOC). The plane-wave cutoff parameter $R_{MT}K_{MAX}$ was set to 7, and the Brillouin zone was sampled by 20,000 k points. Convergence was confirmed by increasing both $R_{MT}K_{MAX}$ and the number of k points until no change in the total energy was observed. The Fermi surface was plotted with the program Crysdien.

III. RESULTS AND DISCUSSION

Fig. 1.(a) shows the temperature dependent resistivity of LaIr_3 from 300 to 2 K. The normal state resistivity shows the poor metallic behavior ($\frac{d\rho}{dT} > 0$) of the polycrystalline sample, with a very low room temperature resistivity. Fig. 1.(b) shows a clear superconducting transition (T_c) of LaIr_3 at 3.3 K and a slightly lower T_c for $\text{LaIr}_{2.8}$ at 2.75 K. We have tested both Ir and La off-stoichiometric effects on the superconducting T_c of this material. La deficiency did not show a strong effect, however Ir deficiency did affect T_c significantly. Fig. 1.(b) shows the effect of Ir off-stoichiometry on T_c . This demonstrates the strong effect of Ir bands around the Fermi level, which is consistent with the band structure calculation studies later discussed in this manuscript. The low-temperature resistivity (above T_c , from 4-25 K)

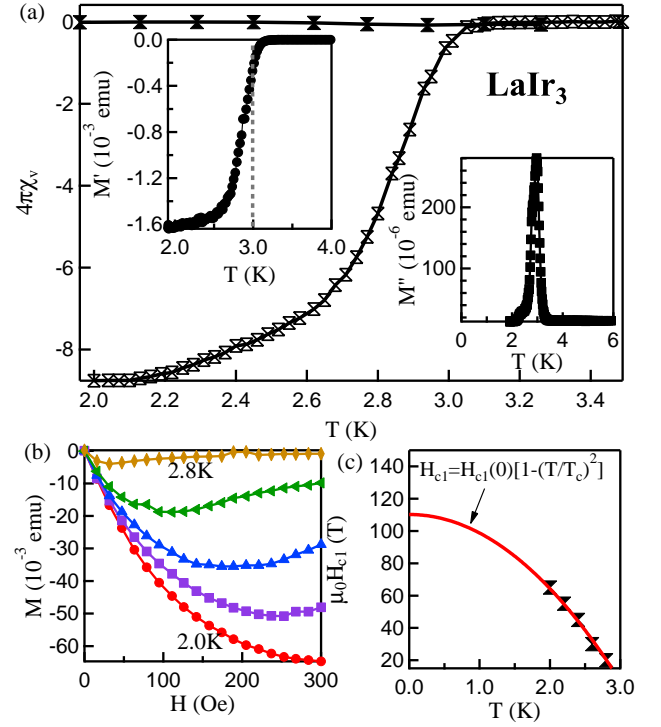


FIG. 2. (Color online) Analysis of magnetization of LaIr_3 . (a) The ZFC and FC DC-magnetization of LaIr_3 . Inset of (a) shows the AC-magnetization. (b) DC-magnetization (M vs. H -curves) at different temperatures from 2K to 2.8K, below the superconducting temperature T_c . (c) The lower critical field as a function of temperature.

data can be described by a power law $\rho = \rho_0 + AT^n$ with $n = 2$, which follows Fermi liquid behavior with the residual resistivity $\rho_0 = 30 \mu\Omega \text{ cm}$, and the coefficient $A = 2.35 \times 10^{-8} \frac{\Omega \text{ cm}}{\text{K}^2}$. The high temperature (above 25 K) data significantly deviates from Fermi Liquid behavior and show a tendency to saturate at higher temperatures. This behavior can be related to the Ioffe-Regel limit [23], when the charge carrier mean free path is comparable to the interatomic spacing and/or to two-band conductivity. [24] Similar behavior was observed for other Ir-based rare earth superconductors, such as CaIr_2 . [8] One measure of the degree of electron correlations in a system is indicated by the value of A , which suggests that LaIr_3 is a weakly correlated electron system. [25] Fig. 1(c) shows the magnetoresistance data for LaIr_3 . The width of the superconducting transition increases slightly with increasing magnetic field. Selecting the 50% normal state resistivity point as the transition temperature, we estimated the orbital upper critical field, $\mu_0 H_{c2}(0)$, from the Werthamer-Helfand-Hohenberg (WHH) expression, $\mu_0 H_{c2}(0) = -0.693 T_c \frac{dH_{c2}}{dT} \big|_{T=T_c}$. A nearly linear relationship is observed in Fig. 1(d) between $\mu_0 H_{c2}$ and T_c . The slope is used to calculate $\mu_0 H_{c2}(0) = 3.84 \text{ T}$. This value of $\mu_0 H_{c2}(0)$ is smaller than the weak-coupling Pauli-paramagnetic limit $\mu_0 H^{Pauli} =$

1.82 $T_c = 6.10$ T for LaIr_3 . We also used the empirical formula $H_{c2}(T) = H_{c2}(0) \left[1 - \left(\frac{T}{T_c} \right)^{\frac{3}{2}} \right]^{\frac{2}{3}}$ to calculate the orbital upper critical field, which yields a value that agrees well with the calculated value using the WHH method. The WHH expression and the empirical formula are widely used to calculate $\mu_0 H_{c2}(0)$ for a variety of intermetallic and oxide superconductors. [3, 8, 26–31, 33] The upper critical field value $\mu_0 H_{c2}(0)$ can be used to estimate the Ginzburg-Landau coherence length $\xi(0) = \sqrt{\Phi_0/2\pi H_{c2}(0)} = 92.59$ Å, where $\Phi_0 = \frac{hc}{2e}$ is the magnetic flux quantum. [34, 35] This value is comparable to the recently reported Laves phase CaIr_2 (see Table. I). [8]

Fig. 2 shows analysis of the magnetization of LaIr_3 . The superconducting shielding fraction can be observed in the zero-field-cooled (ZFC-shielding) and field-cooled (FC-Meissner) data in Fig. 2(a). The bulk superconducting transition $T_c^{\text{onset}} = 3.1$ K can clearly be observed. The very similar values of T_c seen in both resistivity and susceptibility measurements indicate that the polycrystalline sample is homogeneous. Inset of Fig. 2(a) further verifies the superconducting $T_c = 3.1$ K by AC susceptibility. Upper left inset shows real part of AC-susceptibility with $T_c^{\text{onset}} = 3.1$ K and lower right inset shows imaginary part of AC-susceptibility with similar T_c . The magnetization as a function of magnetic field over a range of temperatures below T_c is shown in Fig. 2(b). For analysis of the lower critical field, the point of 2.5% deviation from the full shielding effect was selected for each temperature. Fig. 2(c) shows $\mu_0 H_{c1}$ as a function of T_c . The lower critical field behavior was analyzed with the equation $H_{c1}(T) = H_{c1}(0) \left[1 - \left(\frac{T}{T_c} \right)^2 \right]$. The $\mu_0 H_{c1}$ data are well described with the above equation, and a least squares fit yielded the value of $\mu_0 H_{c1}(0) = 110.24$ Oe, which is much smaller than that of the cubic Laves phase CaIr_2 (see Table. I). [8]

Fig. 3 shows the analysis of specific heat (C) measurements. Fig. 3(a) shows $\frac{C}{T}$ as a function of T , characterizing the specific heat jump at the thermodynamic transition. This jump is completely suppressed under a 5 kOe applied magnetic field. The superconducting transition temperature $T_c = 2.45$ K is shown in the Fig. 3(b), as extracted by the standard equal area construction method. It is not very uncommon to see lower critical temperature from specific heat measurement compare to resistivity measurement, as heat capacity is a bulk measurement, and resistivity and susceptibility can be sensitive to surface super currents that appear at higher temperature. The low temperature normal state specific heat is well fit with the Debye model. The solid line in Fig. 3(c) shows the fitting; the electronic specific heat coefficient $\gamma_n = 11.5 \frac{\text{mJ}}{\text{mol K}^2}$, and the phonon/lattice contribution $\beta_1 = 0.906 \frac{\text{mJ}}{\text{mol K}^4}$ is extracted from the fit. The value of γ obtained is comparable to the cubic Laves phase superconductor CaIr_2 , [8] (which may be due to the fact

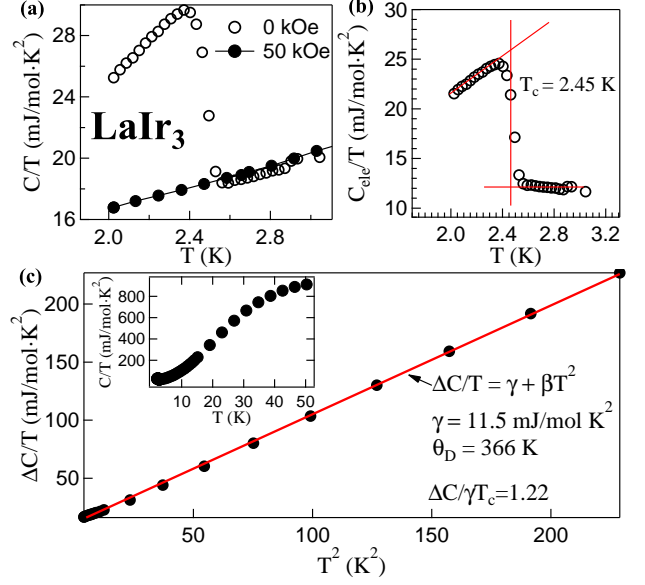


FIG. 3. (Color online) Analysis of heat capacity of LaIr_3 . (a) Heat capacity at zero (open symbol) and 50 kOe (closed symbol) applied field. (b) The electronic heat capacity jump, which can be used to extract T_c by the equal-area construction method. (c) The 50-kOe heat capacity data. The solid line shows the fit with equation $\frac{C}{T} = \gamma + \beta_1 T^2$. The upper left inset shows the zero-field heat capacity as a function of temperature.

TABLE I. Superconducting Parameters of LaIr_3 .

Parameter	Units	LaIr_3
T_c	K	3.32
ρ_0	$\text{m}\Omega\text{cm}$	3.05×10^{-2}
$\frac{dH_{c2}}{dT} _{T=T_c}$	T K^{-1}	-1.67
$\mu_0 H_{c1}(0)$	Oe	110.24
$\mu_0 H_{c2}(0)$	T	3.84
$\mu_0 H^{\text{Pauli}}$	T	6.11
$\mu_0 H(0)$	T	0.0175
$\xi(0)$	Å	92.59
$\lambda(0)$	Å	960
$\kappa(0)$	Å	10.37
$\gamma(0)$	$\frac{\text{mJ}}{\text{mol K}^2}$	11.5
$\frac{\Delta C}{\gamma T_c}$		1.22
Θ_D	K	366
λ_{ep}		0.57
$N(E_F)$	$\frac{eV}{\text{f.u.}}$	0.72

that there are no f orbitals contributing near the Fermi level) and some other Ir-based heavy element superconductors. [3, 13]

The ratio $\frac{\Delta C}{\gamma T_c}$ can be used to measure the strength of the electron-phonon coupling. [36] The specific heat jump $\frac{\Delta C}{T_c}$ for the sample is about $14 \frac{\text{mJ}}{\text{mol K}^2}$, setting

the value of $\frac{\Delta C}{\gamma T_c}$ to 1.22. This is slightly smaller than the weak-coupling limit of 1.43 for a conventional BCS superconductor. The result suggests that LaIr₃ is a weakly electron-phonon coupled superconductor. In a simple Debye model for the phonon contribution to the specific heat, the β coefficient is related to the Debye temperature Θ_D through $\beta = nN_A \frac{12}{5} \pi^4 R \Theta_D^{-3}$, where $R = 8.314 \frac{J}{mol K}$, n is the number of atoms per formula unit, and N_A is Avogadro's number. The calculated Debye temperature for LaIr₃ is thus 366 K. This value of the Debye temperature is slightly higher than that of CaIr₂. [8] An estimation of the strength of the electron-phonon coupling can be derived from the McMillan formula $\lambda_{ep} = \frac{1.04 + \mu^* \ln \frac{\Theta_D}{1.45 T_c}}{(1 - 0.62 \mu^*) \ln \frac{\Theta_D}{1.45 T_c} - 1.04}$. [37, 38] McMillan's model contains the dimensionless electron-phonon coupling constant λ_{ep} , which, in Eliashberg theory, is related to the phonon spectrum and the density of states. This parameter λ_{ep} represents the attractive interaction, while the second parameter μ^* accounts for the screened Coulomb repulsion. Using the Debye temperature Θ_D , critical temperature T_c , and making the common assumption that $\mu^* = 0.15$, [37] the electron-phonon coupling constant (λ_{ep}) obtained for LaIr₃ is 0.57, which suggests weak electron-phonon coupling behavior and agrees well with $\frac{\Delta C}{\gamma T_c} = 1.22$.

The measured magnetic susceptibility of LaIr₃ at 10 K is $\chi = 1.44 \times 10^{-6} \frac{emu}{mol f.u.}$, which can be considered as a spin susceptibility. This allows for an estimate of the Wilson ratio $R_W = \frac{\pi^2 k_B^2 \chi_{spin}}{3 \mu_B^2 \gamma} = 0.21$, which is smaller than that of the free electron value of 1. Also, the coefficient of the quadratic resistivity term can be normalized with the effective mass term from the heat capacity, which results in the Kadowaki-Woods ratio $\frac{A}{\gamma^2}$. This ratio is found to be $0.39 a_0$, where $a_0 = 10^{-5} \frac{m\Omega cm}{(mJ/mol K)^2}$. R_W and $\frac{A}{\gamma^2}$ both indicate that LaIr₃ is a weakly-correlated electron system. [39–41]

The superconducting parameters of LaIr₃ are presented in Table. I.

Fig. 4 shows the analysis of the density of states (DOS) of isostructural LaIr₃ and LaRh₃. The latter is reported to be superconducting at a slightly lower T_c of 2.6 K. [14] It can be clearly observed that the Ir states (Fig. 4(a)) and Rh states (Fig. 4(c)) dominate near the Fermi level, respectively. The contribution of La states is almost negligible at the Fermi level in both systems. Detailed analysis of the DOS calculated with and without SOC shows that it is affecting the LaIr₃ system significantly, but not LaRh₃. To further investigate the effect of SOC, the partial DOS of both systems is plotted in Fig. 4(b) and (d). It can be clearly observed that the Ir-*d* states and Rh-*d* states are dominant near the Fermi level. However, the Ir compound clearly shows a stronger SOC effect, while there is no such effect in the Rh system. This is similar to other Ir based superconducting systems such as CaIr₂. [8] The partial DOS analysis shows that the total DOS is dominated by the contributions from the Ir

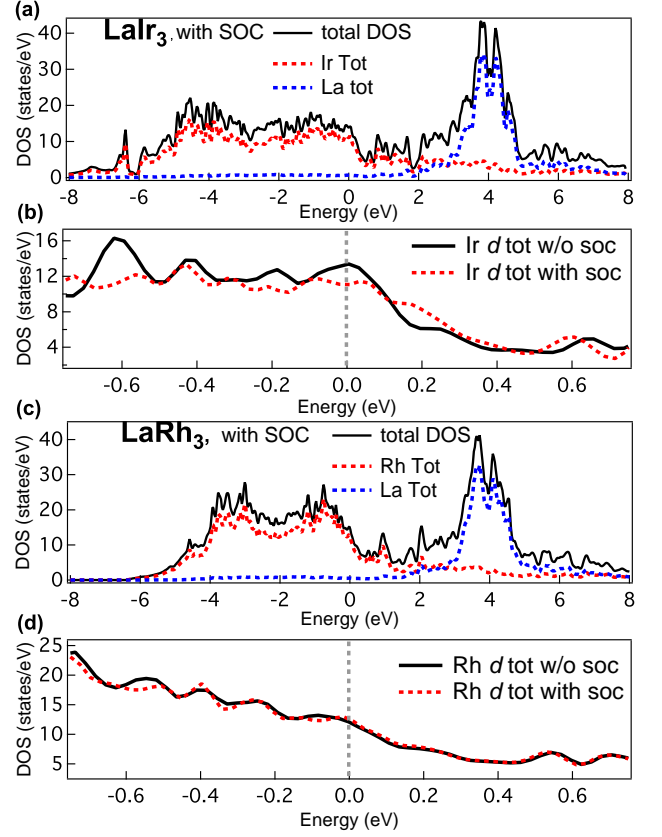


FIG. 4. (Color online) The density of states of LaIr₃ and LaRh₃. (a) The total DOS of LaIr₃, as well as the contributions of La and Ir states respectively. Spin-orbit coupling (SOC) is included. (b) Ir *d*-band DOS with and without SOC. (c) The total DOS of LaRh₃, as well as the contributions of La and Rh states respectively. Spin-orbit coupling (SOC) is included. (d) Rh *d*-band DOS with and without SOC.

sublattice, and that the contribution from the La atoms near the Fermi level is almost negligible. The value of the DOS at E_F (SOC included) is comparable with the value estimated from the heat capacity data. Given the radical change in the Fermi surface (see Fig. 5) due to the spin orbit coupling compared to the hypothetical case where no spin orbit coupling is present, one can speculate that SOC has an effect on the superconducting properties of LaIr₃. This is further strengthened by the fact that T_c is lower in the isostructural Rh analog, where SOC is negligible. LaIr₃ is thus a rare-example of a lanthanide superconductor that is superconducting due the effect of 5*d* electrons.

Fig. 5 shows the calculated band structure of LaIr₃. The SOC effect can be clearly observed near the Fermi level between the Fig. 5(a) and Fig. 5(b). The calculated band structure confirms that LaIr₃ is a three-dimensional metal; several bands with large dispersion cross the Fermi level. The bands at the Fermi level are all derived from Ir 5*d*-orbitals. The arrangement of the Ir lattice should sig-

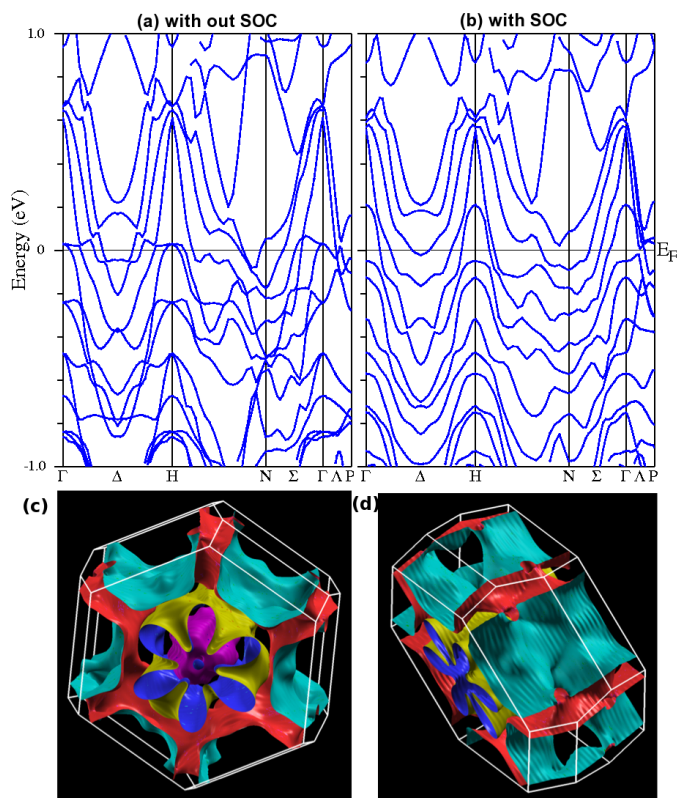


FIG. 5. (Color online) Electronic band structure of LaIr_3 . (a) Band-structure with-out SOC and (b) band-structure with SOC. Complex Fermi surface shows on (c) with-out SOC and (d) with SOC.

nificantly affect the electrons that become superconducting. Similar dispersive bands are observed for the $5d$ -

based cubic laves phase superconductor CaIr_2 . [8] Many bands cross the Fermi energy, therefore the calculated Fermi surface shows complex behavior (See Fig. 5(c) and (d)), and Fig. 5(b) shows the very strong effect of spin-orbit-coupling, which is inherent to Ir- $5d$ states.

IV. CONCLUSION

Here, we have reported the synthesis and characterization of high quality samples of polycrystalline LaIr_3 , which displays superconductivity below $T_c = 3.3\text{K}$. LaIr_3 is a superconductor where the bands near the Fermi surface are dominated by Ir $5d$ states that are strongly affected by SOC. Thus, it is one of the few examples of a lanthanide-based superconductor where $5d$ electrons play the dominate role in the superconductivity. The superconducting parameters obtained from physical properties measurements of LaIr_3 suggest that it is a weakly-coupled BCS-type superconductor. These results motivate future work focused on exploring intermetallic Ir-based superconductors that form in noncentrosymmetric structure types. Strong SOC in these systems would then be antisymmetric, which often leads to exotic and unconventional superconductivity.

V. ACKNOWLEDGMENTS

DPY acknowledges support from the NSF through Grant No. DMR-1306392. NH acknowledges Rowan University research facilities and also acknowledges technical support from Mr. Carl Lunk, Prof. Samuel Loafland and Prof. Jeffery Huttinger.

-
- [1] S. M. Disseler, Chetan Dhital, A. Amato, S. R. Giblin, Clarina de la Cruz, Stephen D. Wilson, and M. J. Graf1, *Phy. Rev. B* **86**, 014428 (2012).
 - [2] R. Movshovich, M. Jaime, J. D. Thompson, C. Petrovic, Z. Fisk, P. G. Pagliuso, and J. L. Sarrao, *Phy. Rev. Lett.* **86**, 5152, (2007).
 - [3] Daigorou Hirai, Mazhar N. Ali, and Robert J. Cava, *J. Phys. Soc. Jpn.* **82** 124701 (2013).
 - [4] Fabian von Rohr, Huixia Luo, Ni Ni, Michael Worle, and Robert J. Cava, *Phy. Rev. B* **89**, 224504 (2014).
 - [5] F. Honda, I. Bonalde, S. Yoshiuchi, Y. Hirose, T. Nakamura, K. Shimizu, R. Settai, and Y. Onuki, *Physica C Superconductivity* **470**, 543 (2010).
 - [6] Daigorou Hirai, Rui Kawakami, Oxana V. Magdysyuk, Robert E. Dinnebier, Alexander Yaresko, and Hidenori Takagi, *Journal of the Physical Society of Japan* **83**, 103703 (2014).
 - [7] T. Klimczuk, F. Ronning, V. Sidorov, R. J. Cava and J. D. Thompson, *Phy. Rev. Lett.* **99**, 257004 (2007).
 - [8] Neel Haldolaarachchige, Quinn Gibson, Leslie M Schoop, Huixia Luo, R. J Cava, *Journal of Physics: Condensed Matter* **27**, 18, 185701 (2015).
 - [9] M. Hakimi and J. G. Huber, *Physica* **135B**, 434-437 (1985).
 - [10] J. G. Huber, *Physica* **163**, 213-229 (1990).
 - [11] Akad, Nauk Ukraiskoi, *Metallofizika* **52**, p121-p123 (1974).
 - [12] A. D. Huxley, C. Paulsen, O. Laborde, J. L. Tholence, D. Sanchez, A. Junod, R. Calemczuk, *J. Phys. Condens. Matter* **5**, 7709 (1993).
 - [13] Hitoshi Sugawara, Hideyuki Sato, Tsuyoshi Yamazaki, Noriaki Kimura, Rikio Settai, and Yoshichika nuke, *J. Phys. Soc. Jpn.* **64**, 4849-4855 (1995).
 - [14] T. H. Geballe, B. T. Matthias, V. B. Compton, E. Corenzwit, G. W. Hull, and D. Longinotti, *Phys. Rev.* **137**, A119 (1965).
 - [15] L. Lutterotti, S. Matthies, H. R. Wenk - IUCr: Newsletter of the CPD, 1999
 - [16] R. A. Hein, J. W. Gibson, B. T. Matthias, T. H. Geballe, and E. Corenzwit, *Phys. Rev. Lett.* **8**, 408 (1962).
 - [17] P. Blaha, K. Schwarz, G. Madsen, D. Kvasnicka and J. Luitz, *WIEN2k, An Augmented Plane Wave + Lo-*

- cal Orbitals Program for calculating Crystal Properties, Technische Universitat Wien, Austria, (2001).
- [18] D. J. Singh, L. Nordstrom, Planewaves, Pseudopotentials, and the LAPW Method, Springer, New York, 2nd ed. (1996).
 - [19] G. K. H. Madsen, P. Blaha, K. Schwarz, E. Sjoestedt, L. Nordstrom, Efficient linearization of the augmented plane-wave method, Phys. Rev. B **64** **19**, 195134 (2001).
 - [20] E. Sjoestedt, L. Nordstrom, D. J. Singh, An alternative way of linearizing the augmented plane-wave method, Solid State Communications **114** 15-20 (2000).
 - [21] J. P. Perdew, K. Burke and M. Ernzerhof, Phys Rev Lett. **77**, 3865 (1996).
 - [22] M. Tinkham, Introduction to Superconductivity, 2nd ed. McGraw Hill, New York (1975).
 - [23] A. F. Ioffe and A. R. Regel, Prog. Semicond. **4**, 237 (1961).
 - [24] V. N. Zverev, A. V. Korobenko, G. L. Sun, D. L. Sun, C. T. Lin, and A. V. Boris, JETP Lett. **90**, 130 (2009).
 - [25] Charles Kittel, Introduction to Solid State Physics, Seventh Edition, John Wiley and Sons, Inc. New York (1996).
 - [26] A. B. Karki, Y. M. Xiong, I. Vekhter, D. Browne, P. W. Adams, K. R. Thomas, H. Kim, R. Prozorov, Julia Y. Chan and D. P. Young, Phys. Rev. B **82**, 064512 (2010).
 - [27] A. B. Karki, Y. M. Xiong, N. Haldolaarachchige, W. A. Phelan, Julia Y. Chan, S. Stadler, I. Vekhter, P. W. Adams, and D. P. Young, Phy. Rev. B, **83**, 144525 (2011).
 - [28] Neel Haldolaarachchige, Quinn Gibson, Jason Krizan, and R. J. Cava, Phy. Rev. B **89**, 104520 (2014).
 - [29] Mazhar N. Ali, Quinn D. Gibson, T. Klimczuk, and R. J. Cava, Physical Review B **89**, 020505(R) (2014).
 - [30] Huixia Luo, Tomasz Klimczuk, Lukas Muchler, Leslie Schoop, Daigorou Hirai, M. K. Fuccillo, C. Felser, and R. J. Cava Physical Review B **87**, 214510 (2013).
 - [31] M. D. Lan, J. C. Chang, K. T. Lu, C. Y. Lee, H. Y. Shih, and G. Y. Jeng, IEEE Transaction on Applied Superconductivity, **11**, 3607-3610 (2001).
 - [32] J. P. Carbotte, Rev. Mod. Phys. **62**, 1027 (1990).
 - [33] Neel Haldolaarachchige, Satya Kushwaha, Quinn Gibson and R. J. Cava, Sup. Cond. Sci. and Tech. **27**, 105001 (2014).
 - [34] N. R. Werthamer, E. Helfand and P. C. Hohenberg, Phys. Rev. **147**, 295 (1966).
 - [35] A. M. Clogston, Phys. Rev. Lett. **09**, 266 (1962).
 - [36] H. Padamsee, J. E. Neighbor, and C. A. Shiffman, J. Low Temp. Phys. **12**, 387 (1973).
 - [37] W. L. McMillan, Phys. Rev. **167**, 331 (1968).
 - [38] Handbook of Superconductivity, edited by C. P. Poole Jr. (Academic Press, New York, 1999), Chap. 9, Sec. G, p. 478.
 - [39] A. C. Jacko, J. O. Fjaerestad and B. J. Powell, Nature Physics **5**, 422 (2009).
 - [40] K. G. Wilson, Rev. Mod. Phys. **47**, 773 (1975).
 - [41] K. Yamada, Prog. Theor. Phys. **53**, 970 (1975).
 - [42] E. Helfand and R. Werthamer, Physical Review **147**, 288-294 (1966).
 - [43] M. Zehetmayer, M. Eisterer, J. Jun, S. M. Kazakov, J. Karpinski, A. Wisniewski, and H. W. Weber, Physical Review B **66**, 252505 (2002).
 - [44] Kazumi Maki, Physical Review **142**, 362-369 (1966).
 - [45] A. Junod, Studies of High Temperature Superconductors, edited by A. Norliker, Nova Science, New York, **19** (1996).
 - [46] N. L. Saini, S. Agrestini, E. Amato, M. Filippi, D. Di Castro and A. Bianconi, Phy. Rev. B **70**, 094509 (2004).
 - [47] M. Higuchi and A. Hasegawa, J. Phy. Sco. Japan **65**, 1302-1211 (1996).
 - [48] Ara Go, William Witczak-Krempa, Gun Sang Jeon, Kwon Park, and Yong Baek Kim, Phy. Rev. Let. **109**, 066401 (2012).
 - [49] Claudia Felser and Ram Seshadri, J. Mater. Chem. **09**, 4597464 (1999).